WEAR PERFORMANCE OF MOORING CHAIN IN WET ENVIRONMENT WITH SUBSTITUTE OCEAN WATER

Gotoh, Koji
Department of Marine Systems Engineering, Faculty of Engineering, Kyushu University

Ueda, Tetsuya
Department of Civil and Structural Engineering, Graduate school of Engineering, Kyushu University : Master course student

Murakami, Koji
Department of Civil and Structural Engineering, Graduate school of Engineering, Kyushu University

Utsunomiya, Tomoaki
Department of Marine Systems Engineering, Faculty of Engineering, Kyushu University

出版情報：Proceedings of the ASME 2019 38th International Conference on Ocean, Offshore and Arctic Engineering: OMAE2019, 2019-11-11. The American Society of Mechanical Engineers : ASME
バージョン：

Proceedings of the ASME 2019 38th International Conference on Ocean, Offshore and Arctic Engineering
OMAE2019
June 9-14, 2019, Glasgow, Scotland, UK

OMAE2019-95822

WEAR PERFORMANCE OF MOORING CHAIN IN WET ENVIRONMENT WITH SUBSTITUTE OCEAN WATER

Koji Gotoh

Department of Marine Systems Engineering,
Faculty of Engineering,
Kyushu University
744 Motooka, Nishi-ku, Fukuoka
819-0395, Japan
E-mail: gotoh@nams.kyushu-u.ac.jp

Tetsuya Ueda
Master course student,
Department of Civil and Structural Engineering,
Graduate school of Engineering,
Kyushu University
744 Motooka, Nishi-ku, Fukuoka
819-0395, Japan
Email: 2TE18310K@s.kyushu-u.ac.jp

Koji Murakami
Department of Civil and Structural Engineering,
Graduate School of Engineering,
Kyushu University
744 Motooka, Nishi-ku, Fukuoka
819-0395, Japan
Email: murakami@nams.kyushu-u.ac.jp

Tomoaki Utsunomiya
Department of Marine Systems Engineering,
Faculty of Engineering,
Kyushu University
744 Motooka, Nishi-ku, Fukuoka
819-0395, Japan
Email: utsunomiya@nams.kyushu-u.ac.jp

ABSTRACT

Floating wind turbine facilities installed in deep sea areas play an essential role in the promotion of green energy. One of the problems associated with the commercialization of facilities installed in the deep sea is the maintenance cost of mooring chains, because they are expensive and wear between links leads to chain breakage. Therefore, it is necessary to establish a quantitative wear evaluation method for mooring chains.

An experimental facility to reproduce the wear caused by sliding between links at the scale of an actual floating wind turbine was developed to investigate the wear performance in seawater conditions, and wear tests were conducted. Substitute ocean water was applied to the experiment instead of seawater. In addition, a procedure for nonlinear finite element analysis was improved to estimate the behaviour of wear between links. Measured stress versus strain relations of the links was considered in the finite element analysis.

The experiments and numerical analysis confirmed that the amount of wear in the substitute ocean water was less than that obtained in dry air and that the tensile force between links is an important factor for the degree of wear between links.

INTRODUCTION

To reduce greenhouse gas emission, renewable energy needs to replace fossil fuels. Wind power generation is expected to play a key role for this goal. The implementation of offshore wind power generation is advantageous because it is capable of stable and efficient power generation due to the strong wind resource that has small variation offshore. To promote offshore wind power generation all over the world, installing floating wind turbine facilities in the deep sea is essential.

One of the challenging issues related to the practical application of a commercialized deep sea facility is the reduction of mooring costs. For example, the mooring chain of floating buoys installed in ports have been damaged owing to wear caused by buoy motion [1]. If the mooring chain of a floating wind power turbine installed in the deep sea breaks owing to wear, this could cause serious damage to the power generation plant. It is essential to establish a method for quantitatively evaluating the wear damage of mooring chains under in-service conditions because current inspection practice is limited to visual inspection by divers or remotely operated vehicles.

Regarding the wear performance of mooring chain, Yaghin and Melchers [2] reported wear test results for stud-link chains with a cross section diameter of 16 mm. In these tests, chain wear was produced by the motion behaviour of mooring chains connected to a floating production storage and off-loading vessels. They confirmed that tensile force working between the links has a significant but non-linear effect on the inter-link wear. Their experiments were, however, slightly small-scale under atmospheric conditions, and they did not describe their procedure for estimating the amount of wear. Brown et al. [3] proposed a practical method to estimate wear and corrosion of mooring chains based on calibration with field measurements. However, the estimate from this method depended on the calibration determined from the specific mooring location.

We previously proposed an experimental facility and numerical nonlinear finite element procedure to reproduce the inter-link wear at actual scale [4][5]. However, our reported experimental and numerical results were under atmospheric conditions. Although it is necessary to investigate the inter-link wear performance in the seawater environment for the safety evaluation of mooring systems, the establishment of an experimental facility for this objective is challenging.

In this study, we developed an experimental facility to achieve an experiment for inter-link sliding wear under wet conditions, rather than underwater, because of the relative simplicity of using such a facility. In addition, we performed nonlinear finite element analysis (FEA) that considered the measured stress versus strain relationship of the material to reproduce inter-link wear.

DEVELOPMENT OF EXPERIMENTAL FACILITY

An experimental facility was proposed [4] and improved [5] to reproduce inter-link wear induced by the motion of the mooring chain. In this study, the experimental facility was modified to study inter-link sliding wear under a wet environment. The specifications of this facility are as follows.

1) Two connected studless link chains were adopted as the test objects.
2) Constant and variable inter-link force can be applied.
3) Constant sliding speed and angle can be applied.
4) Experiments were performed in dry air and wet conditions. In the wet condition, both fresh and substitute ocean water can be used.

An overview of our developed experimental facility is shown in Fig. 1. The test links were connected at location $\boxed{1}$. The left link was mounted horizontally and pulled by hydraulic equipment at location $\boxed{2}$. Sliding movement between the links was achieved by the attached arc-shaped rack and pinion motor, shown at location $\boxed{3}$. The radius of the arc-shaped rack was 588 mm, and the moving arc angle was 90°. One complete motion cycle of the pinion took 243 s. In this improved experimental facility, experimental conditions concerning the inter-link tensile force and the sliding angle can be set for a wide range of values. Apparatus $\boxed{4}$ in this figure is pumping system to drip substitute ocean water onto the inter-link contact region. A drain hole $\boxed{5}$ under the inter-link contact region retrieves water for recirculation by the pumping system $\boxed{4}$.

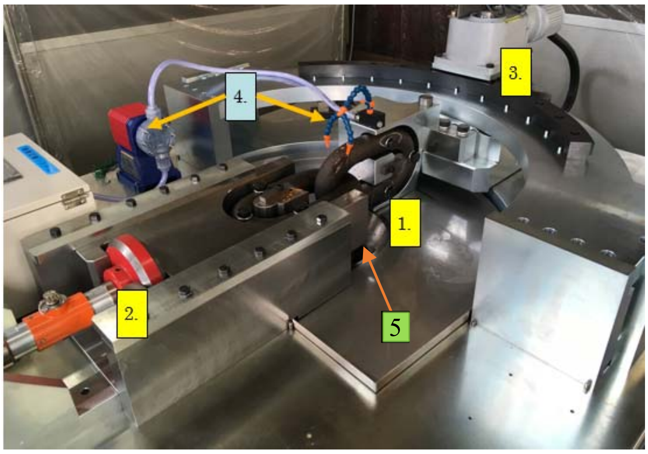

FIGURE 1 OVERVIEW OF MOORING CHAIN WEAR TEST SETUP.

WEAR TEST

Wear tests were performed with studless links made of Grade R3 and R3S classified by the American Bureau of Shipping [6]. The minimum breaking strength of each link was 3,514 kN. The shape of each link is shown in Fig. 2.

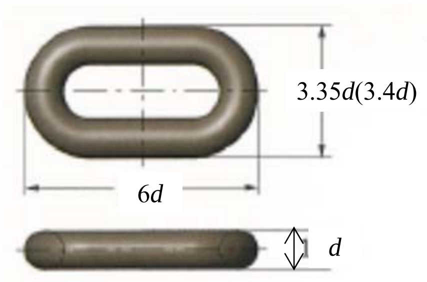

FIGURE 2 SHAPE OF THE STUDLESS LINK (d = 60 mm).

Test conditions are listed in Table 1. To compare the difference of wear performance under wet and dry conditions, some of the experiments were conducted with the same inter-link tensile forces. For the wet condition, substitute ocean water (pH 8.2 at room temperature 15°C) was made according to ASTM D1141 [7] and dripped around the link connection region.

TABLE 1 TEST CONDITIONS.

Material grade	R3			R3S		
Tensile force (kN)	30	20	20	30	30	20
Sliding angle range (deg)	30 (±15)					
Cycle period (s)	82					
Number of cycles	10,000					
Wet (W) or air (A) conditions	W	W	A	W	A	W

The method of collecting wear particles generated during the tests is described below. The collecting tool is illustrated in Fig. 4.

(1) The aluminium tray shown in Fig. 4 (a) was prepared and set in the bottom of water storage tank. This location is under the drain hole $\boxed{5}$ in Fig. 1.
(2) Drain holes were made in the side walls of the tray and covered with paper filters. In addition, double paper filters were placed around the tray, on the bottom of the storage tank, as shown in Fig. 4(b).
(3) Wear particles were captured by the filters. Wear particles that were captured by filters on the tray bottom were collected after the experiment.
(4) After the experiment, all the used paper filters were dried and the weight of these papers was measured.
(5) Total wear weight was identified by subtracting initial paper filter weight from dried paper filter weight after the experiment.

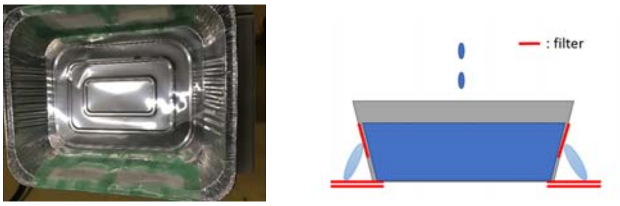

(a) particle collection tray (b) wear particle collecting technique

FIGURE 4 SCHEMATIC ILLUSTRATION OF WEAR PARTICLE COLLECTING TOOL.

WEAR TEST RESULTS

The relationships between the measured total wear weight and number of sliding cycles under the wet condition are shown in Fig. 5. The total wear particle weight for the Grade R3 link is smaller for large inter-link tensile force, but this difference might be ignored because the total wear weight is small and the accuracy of the measurement technique might not be sufficient. Regardless, we confirmed that the wear particle weight is smaller for the stronger material, and that there is no significant difference in particle weight among similar materials.

Figure 6 compares the wear weights for the wet and air conditions. The amount of wear in the air condition was remarkably larger than that in the wet condition when the tensile force was 30 kN. When the tensile force was 20 kN, the difference of wear weight in the air condition is larger than that in the wet condition but still small. These results suggest that the amount of wear in the wet condition is less than that in the air condition. The reason is that water exists between the contact surfaces of links and improves lubricity. In addition, it is confirmed that the effect of inter-link tensile force on the amount of wear is more important than the lubricity of contact surfaces.

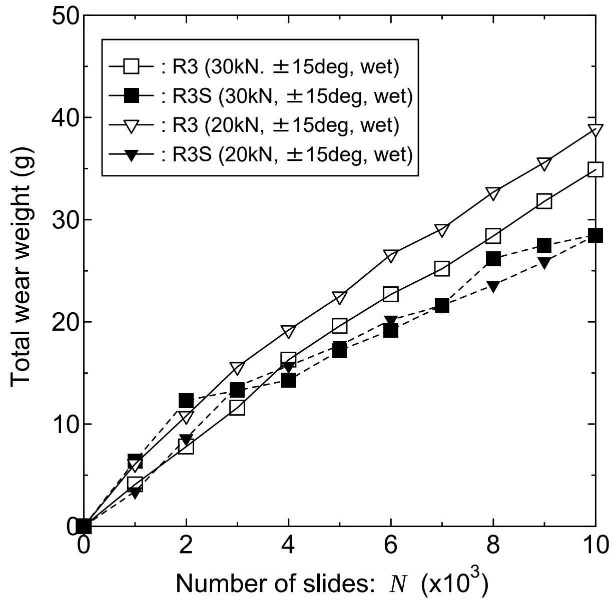

FIGURE 5 COMPARISON OF MEASURED TOTAL WEAR WEIGHT UNDER WET CONDITION.

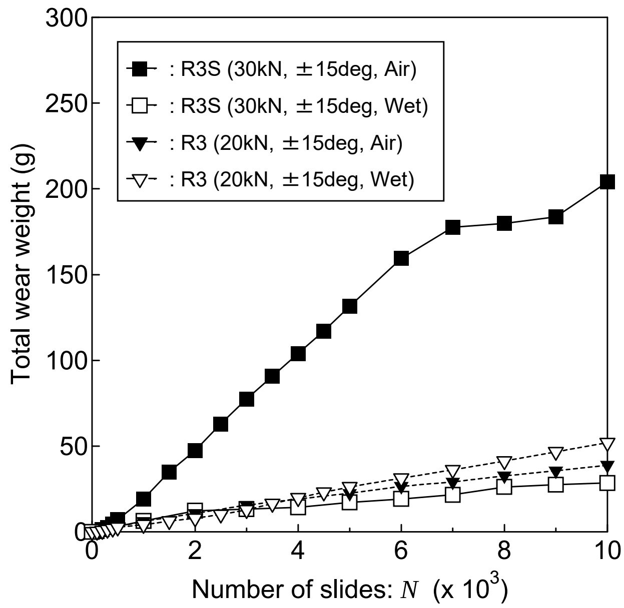

FIGURE 6 COMPARISON OF MEASURED TOTAL WEAR WEIGHT IN WET AND AIR CONDITIONS.

FINITE ELEMENT ANALYSIS TO REPRODUCE THE EXPERIMENT

It is desirable to be able to quantitatively estimate the wear performance at the design stage of floating wind turbines. The tensile force and the sliding angle histories can be estimated by the response analysis for the floating body. Thus, it is expected that the wear behaviour between links can be estimated from the tensile force and sliding range histories derived from the response analysis.

In previous papers [4] [5], the authors showed that inter-link wear behaviour could be reproduced by nonlinear FEA, including element contact effects and a wear function. To perform this FEA, the wear coefficient of the material must be identified. The pin-on-disk wearing test, which is a common wear performance test, was performed to obtain the wear coefficient of the material. The wear coefficients of each material are identified in Table 2 [8] and were applied to the FEA.

TABLE 2 WEAR COEFFICIENT OF CHAIN MATERIALS (mm^2/N).

Condition	R3	R3S
Air	1.1×10^{-3}	1.9×10^{-3}
Wet by substitute ocean water	1.5×10^{-4}	1.3×10^{-4}

The commercial finite element software package Marc 2017 (by MSC) [9] was used in this study. The wear equation proposed by Archard [10] was implemented in Marc 2017 as the governing equation of wear [11].

$$W = \left(K/H\right)\sigma V_{rel} \tag{3}$$

where

W: Wear rate on each finite element node (mm/s),

K: Wear coefficient (mm^2/N),

H : Vickers hardness,

σ: Contact stress on wear surfaces (N/mm^2), and

V_{rel} : Relative sliding speed on contact surfaces (mm/s).

The relationship between stress and plastic strain must be applied to perform nonlinear FEA. However, no quantitative information on this was available; so, we used the bi-linear approximation of this relationship from our previous studies [4] [5]. To improve the accuracy of FEA, the relationship between stress and plastic strain of each link material was measured using advanced non-destructive measuring equipment (AIS 2100) [13] for tensile properties based on the indentation method. The outline of theoretical background of this equipment as follows. The strain hardening coefficient used to describe the plastic flow characteristics of a material is estimated from the characteristic length of the indentation size effect (ISE). There is a linear relationship between the strain hardening index of the sample steels with different plastic pre-strain values and the logarithm of the ISE characteristic length, and it is possible to apply this relationship to estimate the stress-strain curve. Detailed theoretical background is introduced in Ref. [12].

The relationship between true stress and true strain, including the elastic component, yield stress and Young's modulus, can be obtained using this method. Measured results of the relationship between true stress and plastic strain were obtained by subtracting total true strain from the elastic component, as shown in Fig. 7. Other mechanical properties measured by this method are shown in Table 3. Vickers hardness values are also shown in this table, but the measurement was performed separately without using the same indentation method used to obtain values shown in Fig. 7. These values and the density of material 7.85 x 10^{-3} g/mm^3 were applied to the FEA.

TABLE 3 MECHANICAL PROPERTIES OF CHAIN LINKS.

Material grade	R3	R3S
Young's modulus (GPa)	205	296
Yield strength (MPa)	410	462
Density (g/mm^3)	7.85×10^{-3}	
Vickers hardness (Hv)	262	293

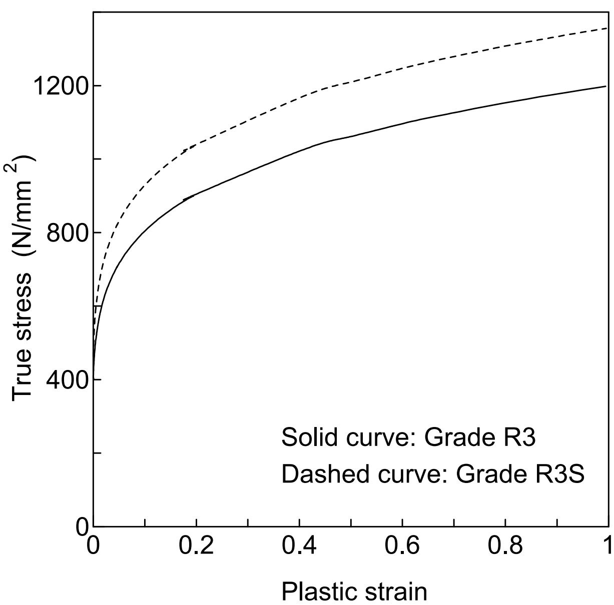

FIGURE 7 MEASURED STRESS VERSUS STRAIN RELATIONS FOR EACH MATERIAL (OBTAINED BY INDENTATION METHOD).

Mesh subdivision and model geometry are shown in Fig. 8. The contact and shape deformation of the bent link section that results from the application of a proof load was considered in the establishment of the FE mesh. This is because the initial proof load could potentially increase the contact area and increase both contact stresses and the wear area [14].

Numerical simulation results are shown in Fig. 9. Some experimental results from the previous section were also plotted in this figure. Because of the limitations of the computer we used (see the PC specifications in Table 4), numerical computation was still ongoing when this paper was submitted. (We will give additional results at the conference.) However, the validity of the FEA could be confirmed from Fig. 9.

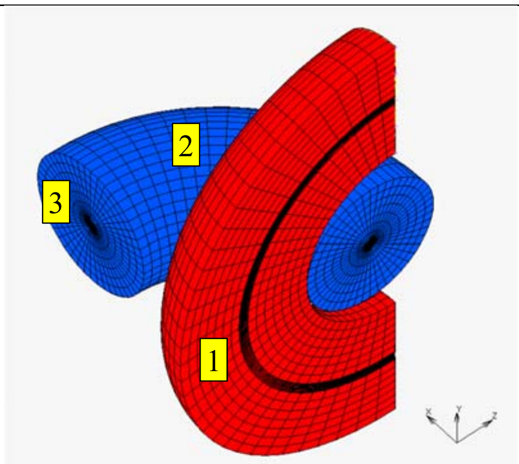

- Number of nodes: 18,759,
- Number of elements: 16,303
- Element size of contact area (x-y-z): 3.9 mm × 3.9 mm × 4.0 mm
- Element type: 8 nodes hexahedral
- Boundary condition:
  - ➢ Fixed x-direction displacement on surface $\boxed{1}$.
  - ➢ Fixed x- and y-direction displacement of the whole blue body.
  - ➢ Tensile loading for z-direction on surface $\boxed{3}$.
- Link sliding method: Rotating body $\boxed{1}$ ±15° around the x-axis with tensile force applied on surface $\boxed{3}$.

FIGURE 8 FINITE ELEMENT SUBDIVISION AND BOUNDARY CONDITIONS.

TABLE 4 SPECIFICATIONS OF COMPUTER.

Operating system	Windows 7 Enterprise, 64-bit
CPU:	Intel® Core™ i7 CPU X980 @ 3.33 GHz
RAM:	22.0 GB

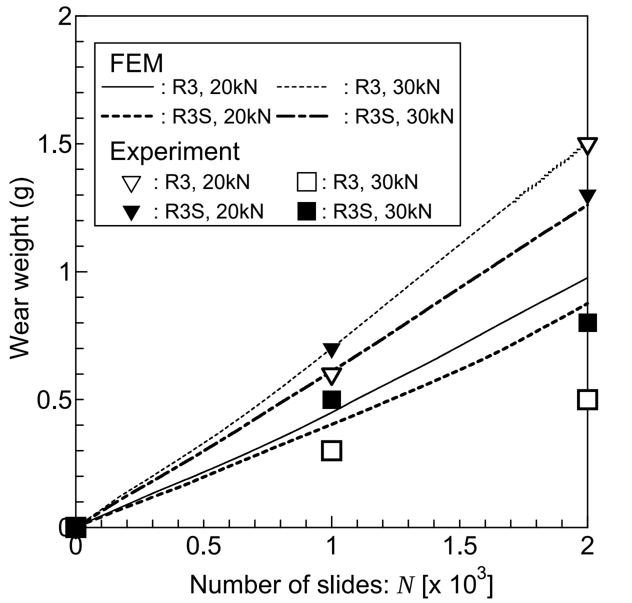

FIGURE 9 COMPARISON OF FE ANALYSIS AND MEASURED RESULT IN WET AND AIR CONDITIONS.

CONCLUSIONS

The experimental facility proposed by the authors in a previous study was improved to reproduce inter-link wear on a realistic scale and to maintain link contact under wet conditions with substitute ocean water or pure water. The experimental results confirmed that the amount of wear in the wet condition is less than that in the dry condition because water increases the lubricity between the contact regions. However, the inter-link tensile force dominates the amount of wear both in wet and dry conditions.

FEA that considered the relationship between true stress and plastic strain of materials was used to reproduce the phenomenon of inter-link wear, and the early stage of the experiment was accurately reproduced.

Future challenges are as follows.

1) Improve the FEA procedure to reproduce the inter-link wear under long periods and variable tensile force and sliding angle conditions.
2) Improve our experimental facility so that the realistic wear test can be performed under the same conditions as an actual in-service mooring chain, in which the contact region is completely submerged.

ACKNOWLEDGMENTS

This research was supported by the Low Carbon Technology Research and Development Program (FY2015-FY2017), Ministry of the Environment, Japan.

Measurement of the relationship between stress and strain was conducted by Dr. Yasushi Morikage (JFE Steel Corp.). The authors express gratitude for his support.

We thank Bryan Schmidt from Edanz Group (www.edanzediting.com/ac) for editing a draft of this manuscript.

REFERENCES

[1] Aso, Y., and Hashimoto, S., 2015, Strength and wear characteristics of the buoy mooring chain, Bulletin of JASNAOE, 62:11-14 (in Japanese).

[2] Yaghim, A.L., and Melchers, R.E., 2015, Long-term inter-link wear of model mooring chains, Marine Structures, 44:61-84.

[3] Brown, M.G., Comley, A.P, Eriksen, M., Williams, I., Smedley, P., Bhattacharjee, S., 2010, Phase 2 Mooring Integrity JIP -Summary of Findings, Proc. OTC, OTC 20613.

[4] Gotoh, K., Murakami, K., Nakagawa, M., and Utsunomiya, T., 2017, Experimental Study on the Wear Performance of the Mooring Chain, Proc. OMAE 2017, OMAE2017-62195.

[5] Gotoh, K., Nakagawa, M., Murakami, K., and Utsunomiya, T., 2018, Effect of Tensile Force for Wear Performance of Mooring Chain, Proc. OMAE 2018, OMAE2018-77960.

[6] American Bureau of Shipping, 1999, Guide for Certification of Offshore Mooring Chain.

[7] ASTM D1141-2013, Standard Practice for the Preparation of Substitute Ocean Water, 2013.

[8] Gotoh, K., Utsunomiya, T., Nakagawa, M., and Yamane, K., 2018, Experimental Study on Specific Wear of Mooring Chain for Floating Structure, J. Japan Society of Naval Architects and Ocean Engineers, Vol. 28 (in press) (in Japanese).

[9] http://www.mscsoftware.com/product/marc (accessed on March 18, 2019).

[10] Archard, J.A., 1956, Contact and Rubbing of Flat Surface, J. Applied Physics, 24:981-988.

[11] MSC Marc 2015 Manual Volume A: Theory and User Information, 2015, pp. 210-212.

[12] Kim, J.Y., Kang, S.K., Greer, J.R., and Know, D., 2008, Evaluating plastic flow properties by characterizing indentation size effect using a sharp indenter, Acta Materialia, 56(14):3338-3343, https://doi.org/10.1016/j.actamat.2008.02.049.

[13] http://www.frontics.com/products/category/27 (accessed on March 18, 2019).

[14] Vargas, P.M., and Jean, P., 2005, FEA of Out-of-Plane Fatigue Mechanism of Chain Links, Proc. OMAE 2005, OMAE2005-67354.

